Research Article

Rapid Communications in Mass Spectrometry

Received: 20 May 2011 Revised: 13 July 2011 Accepted: 21 July 2011 Published online in Wiley Online Library

Rapid Commun. Mass Spectrom. **2011**, *25*, 3131–3145
(wileyonlinelibrary.com) DOI: 10.1002/rcm.5206

Fast screening of highly glycosylated plant sphingolipids by tandem mass spectrometry

Corinne Buré[1]*, Jean-Luc Cacas[2], Fen Wang[2], Karen Gaudin[3], Frédéric Domergue[2], Sébastien Mongrand[2] and Jean-Marie Schmitter[1]

[1]Université de Bordeaux, Chimie Biologie des Membranes et Nanoobjets CBMN – UMR 5248, Centre de Génomique Fonctionnelle Université Bordeaux 2, 146 rue Léo Saignat, 33076 Bordeaux Cedex, France
[2]Université de Bordeaux, Laboratoire de Biogenèse Membranaire, UMR 5200 CNRS-Université Bordeaux Segalen, 146 rue Léo Saignat, 33076 Bordeaux cedex, France
[3]EA 4575 Analytical and Pharmaceutical Developments applied to Neglected Diseases and Counterfeit Drugs, Université Bordeaux Segalen, 146 rue Léo Saignat, 33076 Bordeaux cedex, France

The structural characterization of Glycosyl-Inositol-Phospho-Ceramides (GIPCs), which are the main sphingolipids of plant tissues, is a critical step towards the understanding of their physiological function. After optimization of their extraction, numerous plant GIPCs have been characterized by mass spectrometry. Matrix-assisted laser desorption/ionization mass spectrometry (MALDI-MS) full scan analysis of negative ions provides a quick overview of GIPC distribution. Clear differences were observed for the two plant models studied: six GIPC series bearing from two to seven saccharide units were detected in tobacco BY-2 cell extracts, whereas GIPCs extracted from *A. thaliana* cell cultures and leaves were less diverse, with a dominance of species containing only two saccharide units. The number of GIPC species was around 50 in *A. thaliana* and 120 in tobacco BY-2 cells. MALDI-MS/MS spectra gave access to detailed structural information relative to the ceramide moiety, the polar head, as well as the number and types of saccharide units. Once released from GIPCs, fatty acid chains and long-chain bases were analyzed by GC/MS to verify that all GIPC series were taken into account by the MALDI-MS/MS approach. ESI-MS/MS provided complementary information for the identification of isobaric species and fatty acid chains. Such a methodology, mostly relying on MALDI-MS/MS, should open new avenues to determine structure-function relationships between glycosphingolipids and membrane organization.

In the late 1950s, Carter and collaborators focused their studies on inositol-containing sphingolipids named at the time "phytoglycolipids".[1] The term phytoglycolipid was originally applied to glycolipids containing a phytosphingosine-type long-chain base attached to the inositol-glucuronic acid glucosamine unit by a phosphate ester function. The name 'phytoglycolipid' is obsolete and these compounds have been renamed Glycosyl-Inositol-Phospho-Ceramides (GIPCs).[2–4] GIPCs are only found in plants and fungi but not in animals or bacteria.[3–8] Complex glycophosphosphingolipids account for both free GIPC and protein-bound GIPC anchors. They represent the major sphingolipids in plant membranes.[9] By contrast, sphingomyelin, which has a phosphocholine head group, is the major phosphosphingolipid in animal tissues, but has not been detected in plants. Noteworthy, while sphingolipids such as monohexosylceramides are conserved among kingdoms, non-phosphorous oligoglycosphingolipids including cerebrosides and gangliosides are specific to the animal phyllum.

* *Correspondence to:* C. Buré, Chimie Biologie des Membranes et Nanoobjets CBMN – UMR 5248 Centre de Génomique Fonctionnelle BP 68, Université Bordeaux 2, 146 rue Léo Saignat, 33076 Bordeaux cedex, France.
E-mail: c.bure@cbmn.u-bordeaux.fr

Although GIPCs belong to one of the earliest identified classes of plant sphingolipids, to date only a few GIPCs have been fully characterized.[1,10–13] This is mainly due to their high polarity and relatively poor extraction yield using classic techniques.[2,9,14] Indeed, solubilization of GIPCs has been a major obstacle to their study. Most techniques use a chloroform/methanol mixture and phase partition for lipid extraction, but this is inefficient for GIPCs that remain either in the aqueous phase or at the interphase, or even end up in the insoluble pellet.

GIPCs possess a glucuronic acid-inositol-phosphate-ceramide core structure, to which additional sugar units may be attached, forming structures such as Gal-GlcN-GlcA-inositol-1-phosphate-ceramide and GlcN-GlcA-inositol-1-phosphate-ceramide (where Gal is galactose, GlcN glucosamine and GlcA glucuronic acid).[5,10,13] Long-chain base (LCB) profiles of GIPCs are dominated by t18:0 (t standing for trihydroxylated; this compound is called phytosphingosine) and t18:1 species in widely varying proportions (for review, see Pata *et al.*[15]).

The objective of this work was the design of a mass spectrometric approach that could provide a quick, but complete description of GIPC species occurring in plants. Matrix-assisted laser desorption/ionization (MALDI) in the negative ion mode, using a tandem instrument that can deliver both accurate mass measurements and informative fragment ion spectra from singly charged precursor ions, was the method

of choice. Electrospray ionization (ESI) was used to provide complementary structural information via tandem mass (MS/MS) spectra of doubly charged species, and some isobaric species were differentiated in this way. Fatty acid chains and LCBs were released from sphingolipids and analyzed by gas chromatography/mass spectrometry (GC/MS) to verify that all GIPC series were taken into account by the MALDI-MS/MS approach. For this purpose, GIPC-released fatty acid chains were submitted to transesterification and trimethylsilylation, and LCBs were transformed into fatty aldehydes after periodate oxidation.

Besides *Arabidopsis* plants, an essential model for reverse/forward genetic and physiological approaches, *Arabidopsis* and tobacco suspension cells were also chosen as models because they represent a widely used material for subcellular fractionation, *in vivo* imaging, signal transduction and plant defense studies.[16,17] Furthermore, GIPCs are likely located in the plasma membrane,[15] which is probably the most diverse membrane of the cell with a protein and lipid composition varying with cell type, developmental stage, and environment. In this respect, using an undifferentiated cell suspension as starting material is an advantage.

EXPERIMENTAL

Plant materials

Wild-type tobacco BY-2 cells (*Nicotiana tabacum* cv. Bright Yellow 2) were grown as previously described.[18] *Arabidopsis thaliana* cells (accession *Landsberg erecta*) were grown as previously described.[19] Seven-day-old cell cultures were used for GIPC extraction (see next section). *Arabidopsis thaliana* plants were in the Columbia (Col-0) ecotype background. For experimental analyses, sterilized seeds were sown on MS (Murashige and Skoog) medium supplemented with 0.7% agar. The seeds were stratified in the dark for 3 to 4 days at 4 °C and then transferred to long-day conditions (16 h light/8 h dark cycle) at 22 °C or continuous light conditions at 20 °C. Seedlings were transferred 10 days to 3 weeks later to a soil-vermiculite mixture and further grown at 20 to 22 °C under long-day conditions.

Extraction and purification of GIPCs

GIPCs were purified according to a method adapted from Carter and Koob[10] to obtain final amounts in the milligram range. Briefly, plants cells (ca. 100–200 g of fresh weight) were blended with 400 mL cold 0.1 N aqueous acetic acid in a chilled Waring Blendor at maximum speed for 2 min. The slurry was filtered under vacuum through 16 layers of acid-washed miracloth on a large funnel. The residue was extracted twice again in the same manner. The aqueous acetic acid filtrate was discarded and the residue was then re-extracted with hot (70 °C) 70% ethanol containing 0.1 N HCl. The slurry was filtered hot through miracloth and washed with acidic 70% ethanol. The residue was re-extracted twice more with acidic 70% ethanol. The combined filtrates were chilled immediately and left at −20 °C overnight. The precipitate was pelleted by centrifugation at 2000 *g* at 4 °C for 15 min. The GIPC-containing pellet was washed with cold acetone until washes were colorless, and finally with cold diethyl ether to yield a whitish precipitate. The typical yield of this crude extract was 0.2–0.5% of the fresh weight starting material. GIPCs were then dissolved in tetrahydrofuran (THF)/methanol/water (4:4:1, v/v/v) containing 0.1% formic acid by heating at 60 °C, followed by gentle sonication. GIPC extracts were further dried and submitted to a butan-1-ol/water (1:1, v/v) phase partition. This process left proteins and cell walls in the lower aqueous phase, whereas more than 97.5% of the GIPCs were recovered in the upper butanolic phase, as determined by quantitative GC/MS analysis. Finally, the latter phase was dried and the residue was dissolved in THF/methanol/water (4:4:1, v/v/v) containing 0.1% formic acid. This solution was further used for MS analysis.

Fatty acid analysis

Samples (representing approximately 0.25% of the total amount, i.e. 250 mg of fresh weight or 25 mg dry weight) were spiked with 50 µg heptadecanoic acid (17:0) and 50 µg 2-hydroxyltetradecanoic acid (h14:0) as internal standards, and transmethylated overnight at 85 °C in 1 mL methanol containing 5% sulfuric acid (v/v). Upon cooling, 1 mL of NaCl (2.5%, w/v) was added and released fatty acid methyl esters (FAMEs) were extracted in hexane. The organic phase was then washed with 1 mL of saline solution (250 mM NaCl and 250 mM Tris, pH 8.0), gently dried under a nitrogen stream, dissolved in 100 µL of *N,O*-bis(trimethylsilyl)trifluoroacetamide with trimethylchlorosilane (BSTFA-TMS, Sigma-Aldrich) and heated at 110 °C for 15 min to derivatize free hydroxyl groups. Remaining BSTFA-TMS was evaporated under nitrogen and samples were dissolved in hexane for GC/MS analysis. An HP-5MS capillary column (5% phenyl-methyl-siloxane, 30 m × 250 µm, 0.25 µm film thickness; Agilent) was used with helium carrier gas at 2 mL/min; injection was in splitless mode; injector and MS detector temperatures were set to 250 °C; the oven temperature was held at 50 °C for 1 min, then programmed with a 25 °C/min ramp to 150 °C (2 min hold), and a 10 °C/min ramp to 320 °C (6 min hold). Quantification of fatty acids and their hydroxylated counterparts was based upon peak areas that were derived from the total ion current (TIC).

Long-chain base analysis

Long-chain base content of sphingolipids was determined using a previously described method that relies on periodate oxidation of free LCBs into their corresponding fatty aldehydes.[20] The latter can be readily quantified by GC/MS. Before oxidation, LCBs were released from sphingolipids by warming up at 110 °C for 16 h in a solution containing 1 mL barium hydroxide (10%, w/v) and 1 mL dioxane (Sigma-Aldrich). GC conditions were identical to those described above for fatty acid analysis. Samples represented approximately 0.25% of the total amount, i.e. 250 mg of fresh weight or 25 mg dry weight. Internal standards were d20:0 and t17:0 (representing 2-aminoeicosane-1,2-diol and 2-aminoheptacosane-1,2,4-triol, respectively), purchased from Sigma-Aldrich and Avanti Polar Lipids.

Methylamine treatment

The methylamine working solution was prepared by mixing (7:3, v/v) a 33% methylamine ethanolic solution (Sigma-Aldrich) with a 41% methylamine aqueous solution (Fluka

Rapid Communications in Mass Spectrometry

Analytical). The sphingolipid-containing powder was directly dissolved in the methylamine working solution and incubated at 50 °C for 1 h. Samples were dried under nitrogen and sphingolipids were redissolved in THF/methanol/water (4:4:1, v/v/v) containing 0.1% formic acid as described earlier.[21] This treatment does not affect the amide bonds of sphingolipids, as confirmed by the analysis of standard sphingolipids, including sphingomyelin from bovine brain (Sigma-Aldrich) and soybean glucosylceramide (Avanti Polar Lipids) (data not shown). Samples destined for MS analysis were not treated with methylamine to avoid any ion adduct formation that could interfere with MS analysis.

MALDI-MS and -MS/MS

A saturated solution of 2,6-dihydroxy-acetophenone (DHA) matrix (Aldrich) was prepared in 50:50 (v/v) ethanol/water containing 3 mM ammonium sulfate.[22] GIPC sample concentration was 0.5 mg/mL in THF/methanol/water (4:4:1, v/v/v) containing 0.1% formic acid. Samples (0.5 µL representing approximately 0.125% of the total amount, i.e. 12.5 mg of starting fresh weight) were mixed with matrix solution (0.5 µL) before being loaded on the MALDI plate.

Spectra were acquired in negative ion mode on a MALDI Q-ToF mass spectrometer (QToF Premier; Waters, Manchester, UK). The laser was set to an energy level of 250 on the instrument scale. The mass range was from *m/z* 800 to 3000. Ganglioside GM1 from ovine brain (Avanti Polar Lipids) was used for near point calibration (lock mass, *m/z* 1545.8767). MS/MS experiments were achieved with a collision energy of −40 to −80 eV on a compound-dependent basis.

ESI-MS and -MS/MS

GIPC extracts were diluted 16-fold in 65:35 (v/v) isopropanol/water containing 0.03% ammonium acetate. Each sample was infused into the TurboV electrospray source of a QTRAP 5500 mass spectrometer (AB Sciex, Concord, Ontario, Canada) at a flow rate of 7 µL/min^{-1}. ESI-MS/MS experiments were performed in negative ion mode, with a curtain gas (nitrogen) of 15, gas1 (nitrogen) set to 20, gas2 (nitrogen) set to 0, needle voltage at −4500 V without needle heating, declustering potential at −100 V and a scan rate of 1000 Da/s. Calibration was achieved using an ES Tuning Mix (AB Sciex).

The collision gas was nitrogen. The collision energy was varied from −40 to −60 eV on a compound-dependent basis. The mass range (*m/z* 50–1000) was scanned with a dwell time between 0.05 and 0.7 s depending of the ion mass. In general, collision-induced dissociation (CID) spectra represent summations of about 48 scans.

RESULTS

Purification of plant GIPCs and characterization of their ceramide moieties

Some 60 years ago, Carter and Koob described a method dedicated to the purification of phytoglycolipids.[10] Later on, Kaul and Lester reported on a similar procedure for the isolation of phytoglycolipid-related molecules, known as phytosphingolipids.[11] We have re-explored and slightly modified the original protocol for phytoglycolipid purification to make it suitable for mass spectrometric analysis of GIPCs (Fig. 1). Modifications merely consisted of (i) getting rid of proteins and (ii) finding a solvent for GIPCs that is compatible with MALDI and ESI experiments. A two-phase partition step with a 1:1 (v/v) water/butan-1-ol mixture was found to be optimum for GIPC recovery without protein contamination. Based on the aforementioned criterion, an acidic THF/methanol/water (4:4:1, v/v/v) solution was chosen for solubilization of GIPCs.

Quantitative analysis of FAs and LCBs released from sphingolipids

As a complement to the screening of intact GIPCs in MALDI and ESI ionization modes, more information was sought by examination of the FA and LCB contents of GIPCs.

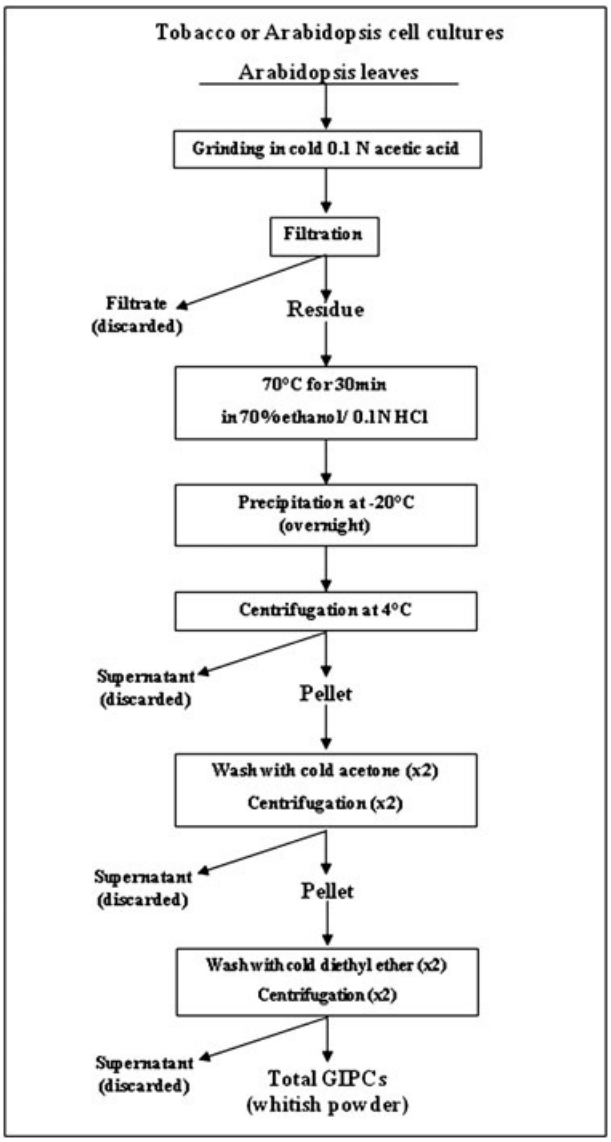

Figure 1. Purification of BY2 and *A. thaliana* GIPCs. GIPC purification scheme, adapted from Carter and Koob.[10] GIPCs were purified from 7-day-old *Nicotiana tabacum* (BY-2) and *Arabidopsis thaliana* (accession *L. erecta*) cell cultures and leaves.

FA chains of GIPCs were analyzed after methylamine treatment, to eliminate contaminating ester-bond-containing lipids such as galactolipids and phospholipids.[21] Before GC analysis, samples were transmethylated under acidic conditions and then trimethylsilylated; the latter step was intended for quantitative analysis of 2-hydroxylated FAs (see Experimental section).

After methylamine treatment, 16 and 18 carbon-atom-long fatty chains were not found in GIPC samples, and only very long-chain fatty acids (VLFCAs, more than 20 carbon atoms) and 2-hydroxylated 16 carbon-atom-long fatty acids were detected (see Fig. 2(b)). FA profiles were markedly different in the three plant tissues. Tobacco cell culture GIPCs exhibited an equally high content of VLCFA and their 2-hydroxylated counterparts, behenic (22:0) and lignoceric (24:0) acids, together with h22:0 and h24:0 being the major molecular species (Fig. 2). 24:0 appeared to be the major VLCFA in *Arabidopsis* cell culture with h24:0 the second most abundant one (50 and 20 mol%, respectively). By contrast, 2-hydroxylated VLCFAs were the major FAs in *Arabidopsis* leaf GIPCs, with about 5 mol% of 2-hydroxylated 16:0 which was hardly detectable in cell culture. The VLCFA profile of *Arabidopsis* leaf GIPCs with mostly 2-hydroxylated FA chains is in agreement with previously published results,[14,21] and is also observed in tobacco leaves (data not shown).

LCBs were released from sphingolipids by treatment with barium hydroxide at 110 °C and transformed into aldehydes by periodate-mediated oxidation, as described in the Experimental section.[20] Quantification of LCBs was carried out

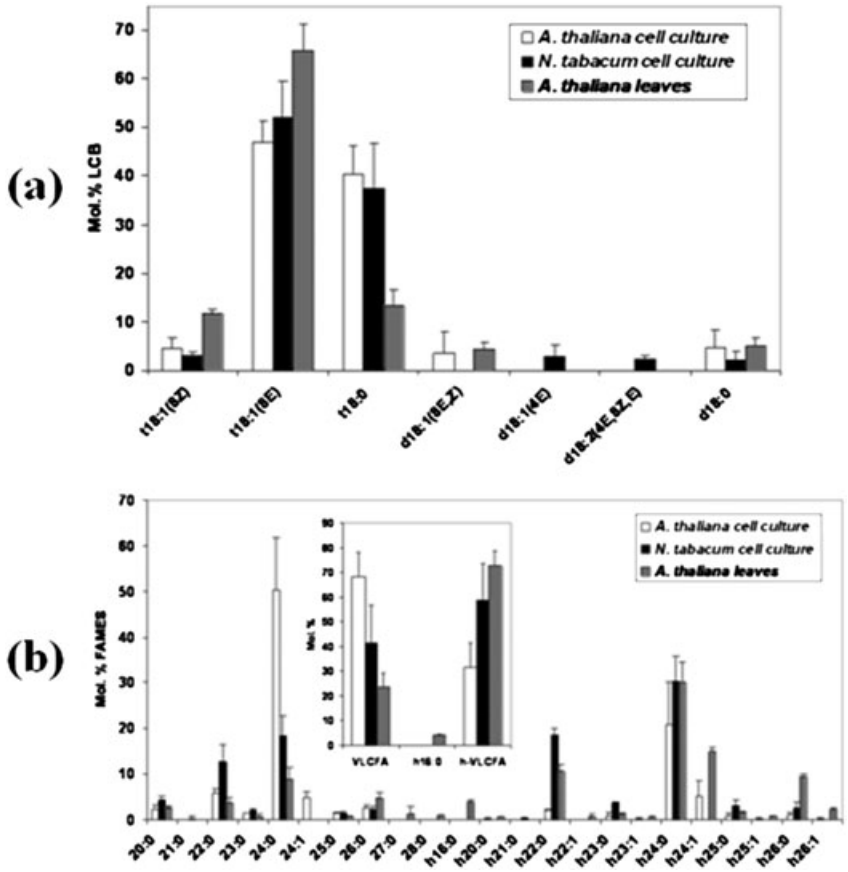

Figure 2. Characterization of GIPC ceramide moieties. (a) Long-chain base (LCB) content of GIPCs was determined as described in the Experimental section. Three independent samples were processed (mean and SD). LCB nomenclature is based upon the 2-aminoacyl backbone of the molecules. Hence, t18:0 represents 2-aminooctadecane-1,2,4-triol (trivial name phytosphingosine); t18:1(8*Z*) represents 2-aminooctadec-8(*Z*)-ene-1,2,4-triol (trivial name, (8*Z*)-phytosphingenine); t18:1(8*E*) represents 2-aminooctadec-8(*E*)-ene-1,2,4-triol (trivial name, (8*E*)-phytosphingenine); d18:1(4*E*) represents 2-aminooctadec-4(*E*)-ene-1,2-diol (trivial name (4*E*)-sphingenine or sphingosine); d18:1(4*Z*) represents 2-aminooctadec-4(*Z*)-ene-1,2-diol (trivial name (4*Z*)-sphingenine); d18:2(4*E*,8*Z*) represents 2-aminooctadeca-4,8(*E*,*Z*)-dienine-1,2-diol (trivial name (4*E*,8*Z*)-sphingadienine); d18:2(4*E*,8*E*) represents 2-aminooctadeca-4,8(*E*,*E*)-dienine-1,2-diol (trivial name (4*E*,8*Z*)-sphingadienine); d18:0 represents 2-aminooctadecane-1,2-diol (trivial name sphinganine or dihydrosphingosine). Internal standards were d20:0 and t17:0 (representing 2-aminoeicosane-1,2-diol and 2-aminoheptacosane-1,2,4-triol, respectively). (b) Fatty acid content of GIPCs. FAs were released from lipids by acid methanolysis; the resulting FAMEs were subsequently derivatized with BSTFA before GC/MS analysis. Three independent samples were processed (mean and SD).

by GC/MS, using 2-aminoeicosane-1,2-diol and 2-aminoheptacosane-1,2,4-triol as internal standards.

LCB distributions were quite similar for all plant models. In accordance with previous reports, we found that the two major LCBs were trihydroxylated compounds, irrespectively of the plant species (Fig. 2(a)).[5,13,14] Phytosphingosine (t18:0), an LCB conserved among plant and fungi kingdoms, and its trans-unsaturated counterpart (t18:1^{8E}), represented nearly 90% of total LCBs (Fig. 2(a)). In *Arabidopsis* leaf GIPCs, mostly t18:1 was detected, as previously described by Markham *et al*.[14,21] Minor LCBs, mainly dihydroxylated ones, were more plant model specific species. For instance, while d18:1^{8E} was only present among *Arabidopsis* GIPCs, sphingosine (d18:1^{4E}) and d18:2^{4E,8Z,E} were exclusively found among BY-2 GIPCs (Fig. 2(a)).

GIPC screening by MALDI-MS

Several matrices (alpha-cyano-4-hydroxycinnamic acid, 2,5-dihydroxybenzoic acid, 2,4,6-trihydroxyacetophenone, 3-hydroxypicolinic acid and 2,6-dihydroxyacetophenone) were tested with plant lipid extracts in positive and negative ion modes (data not shown). By far the best result in terms of sensitivity was obtained with 2,6-dihydroxyacetophenone (DHA) in the negative ion mode, with the observation of the sole $[M–H]^-$ ionic species. MALDI mass spectra of BY-2 cell culture, *A. thaliana* cell culture and leaf samples are shown in Figs. 3(a), 3(b) and 3(c), respectively. The comparison of these spectra reveals several clusters of compounds in different mass ranges, i.e. series A from *m/z* 1200 to 1340, series B from *m/z* 1370 to 1470, series C from *m/z* 1500 to 1580, series D from *m/z* 1640 to1750, series E from *m/z* 1790 to 1910, and series F from *m/z* 1930 to 2040. In *A. thaliana* cells and leaves as well as BY-2 cells, each series is composed by several species differing from one another by 2, 14 and 16 Da, corresponding to various numbers of unsaturation, carbon atoms and hydroxylation of the fatty acid chain, respectively. In *A. thaliana* cells and BY-2 cells, the spacing between series is either 162 or 132 Da, corresponding to the addition of a hexose or pentose unit. Thus, the observed GIPC series bear a variable number of saccharide units, from two in series A up to seven in series F (Figs. 3(a) and 3(b)).

Major GIPC peaks were partly characterized by means of accurate mass measurements with the MALDI-Q-ToF mass spectrometer on the basis of structures already reported in the literature. Indeed, major GIPCs from tobacco and *A. thaliana* leaves were identified as hexose(R1)-hexuronic acid-inositol-phosphoceramide;[5,13,14] these GIPCs correspond to the major compounds of series A in our study. In *A. thaliana* leaves, the ceramide moiety was identified as t18:1 h24:0[14] or t18:1 h24:1[21] with R1 as a hydroxyl group. Similarly, a h24:0 fatty acid chain was found in GIPCs from tobacco leaves, with an amine or an acetylamine for R1.[13,15]

Assigned structures within series A to F are listed in Table 1. In extracts from *A. thaliana* leaves and cells and BY-2 cells, we observed GIPC species differing from one another by 14 Da, mainly in series A, suggesting the occurrence of fatty acid chains with odd and even carbon numbers. This finding was confirmed by GC/MS analysis of fatty acids (Fig. 2(b)). In *A. thaliana* leaves, only compounds belonging to series A were observed. The most intense peaks were found at *m/z* 1258.71 ($[M–H]^-$ ion), corresponding to a hexose(R1:OH)-hexuronic acid-inositol-phosphoceramide having a t18:1 h24:1 ceramide moiety (theoretical *m/z* 1258.74), and at *m/z* 1260.72 ([M-H]$^-$ ion), corresponding to a hexose(R1:OH)-hexuronic acid-inositol-phosphoceramide having a t18:1 h24:0 ceramide moiety

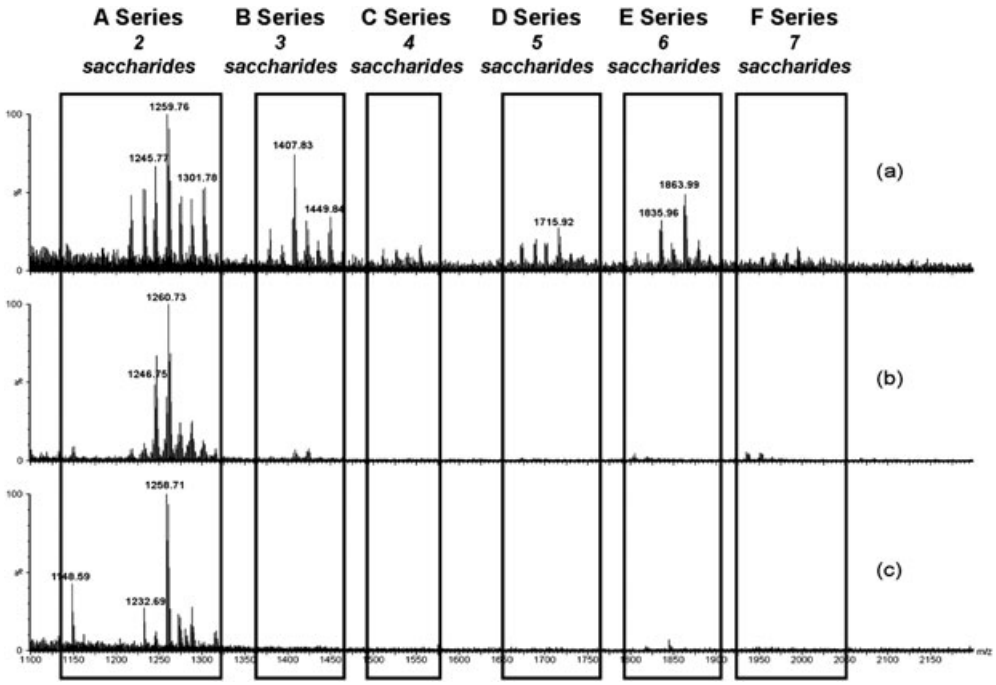

Figure 3. MALDI-MS analysis of GIPC extracts (a) from BY-2 cells, (b) from *A. thaliana* cells, and (c) from *A. thaliana* leaves. Spectra were acquired in the negative ion mode using 2,6-dihydroxyacetophenone (DHA) as a matrix. GIPCs are grouped in series according to their number of saccharide units, from two (series A) to seven (series F).

Table 1. Experimental and theoretical mass values for GIPCs belonging to series A to F

	LCB	FA	*A. thaliana* leaves		*A. thaliana* cells		BY-2 cells		BY-2 cells	
			Experimental $[M-H]^-$	Theoretical $[M-H]^-$	Experimental $[M-H]^-$	Theoretical $[M-H]^-$	Experimental $[M-H]^-$	Theoretical $[M-H]^-$	Experimental $[M-H]^-$	Theoretical $[M-H]^-$
Series A structures			**Glc-GlcA-Ins-P-Cer**		**Glc-GlcA-Ins-P-Cer**		**GlcN-GlcA-Ins-P-Cer**		**GlcNAc-GlcA-Ins-P-Cer**	
	t18 :0	**20:0**							1231.72	1231.71
		21:0							1245.77	1245.72
		22 :1					1215.72	1215.71		
		22 :0					1217.74	1217.73	1259.76	1259.74
		23 :0					1231.72	1231.74	1273.75	1273.75
		24 :1					1243.75	1243.74		
		24 :0	1246.71	1246.74	1246.75	1246.74	1245.77	1245.76	1287.78	1287.77
		25 :0					1259.76	1259.78	1301.78	1301.79
	t18:0	**h16:0**	1150.60	1150.61	1150.62	1150.61				
		h19:0							1233.72	1233.69
		h21:0							1261.77	1261.72
		h22 :0					1233.72	1233.72	1275.75	1275.73
		h23 :1	1246.71	1246.71	1246.75	1246.71				
		h23 :0			1248.75	1248.72			1289.78	1289.75
		h24 :0	1262.73	1262.74	1262.75	1262.74	1261.77	1261.75	1303.78	1303.77
		h25 :1	1274.73	1274.74	1274.75	1274.74				
		h25 :0			1276.75	1276.75				
		h26 :1	1288.75	1288.76	1288.77	1288.76				
		h26 :0	1290.74	1290.77						
		h28 :1	1316.79	1316.79						
	t18 :1	**21 :0**							1243.75	1243.71
		22 :0					1215.72	1215.71		
		24 :0	1244.70	1244.73	1244.74	1244.73	1243.75	1243.74		
		25 :0	1258.71	1258.74	1258.72	1258.74				
		26 :0	1272.72	1272.76	1272.75	1272.76				
		27 :0	1286.74	1286.78	1286.75	1286.78				
		29 :0	1314.77	1314.81						
	t18:1	**h16:0**	1148.59	1148.60	1148.60	1148.60				
		h20:1							1243.75	1243.67
		h20:0							1245.77	1245.69
		h21:1					1215.72	1215.68		
		h21:0					1217.74	1217.69	1259.76	1259.70
		h22 :0	1232.69	1232.69	1232.71	1232.69	1231.72	1231.71	1273.75	1273.72
		h23:1	1244.70	1244.69	1244.74	1244.69	1243.75	1243.71	1285.73	1285.72
		h23 :0	1246.71	1246.71	1246.75	1246.71	1245.77	1245.72	1287.78	1287.73
		h24 :1	1258.71	1258.71	1258.72	1258.71				

(*Continues*)

		h24 :0	1260.72	1260.72	1260.73	1260.72	1259.76	1259.74	1301.78	1301.75
		h25 :1	1272.72	1272.72	1272.75	1272.72				
		h25 :0	1274.73	1274.74	1274.75	1274.74				
		h26 :1	1286.74	1286.74	1286.75	1286.74				
		h26 :0	1288.75	1288.76	1288.77	1288.76				
		h28 :1	1314.77	1314.77						
		h28 :0	1316.79	1316.79						
Series B structures					**Hex-Glc-GlcA-Ins-P-Cer**		**Hex-GlcN-GlcA-Ins-P-Cer**		**Hex-GlcNAc-GlcA-Ins-P-Cer**	
	t18 :0	**22 :0**					1379.79	1379.78	1421.81	1421.79
		23 :0					1393.79	1393.80	1435.84	1435.81
		24 :0			1408.79	1408.80	1407.83	1407.81	1449.84	1449.82
		25 :0			1422.79	1422.81	1421.81	1421.83		
		26 :0					1435.84	1435.84		
		27 :0					1449.84	1449.86		
	t18 :0	**h21:1**					1379.79	1379.75		
		h21:0							1423.82	1423.77
		h22 :0					1395.77	1395.78	1437.83	1437.79
		h23 :1			1408.79	1408.76	1407.83	1407.78		
		h23 :0			1410.78	1410.78	1409.83	1409.79	1451.86	1451.80
		h24 :1			1422.79	1422.78				
		h24 :0			1424.8	1424.79	1423.82	1423.81		
		h25 :0			1438.77	1438.81	1437.83	1437.82		
		h26 :0					1451.86	1451.84		
	t18 :1	**22 :0**					1377.77	1377.77	1419.81	1419.78
		23 :0					1391.76	1391.78	1433.84	1433.79
		24 :0			1406.79	1406.78	1405.81	1405.80	1447.81	1447.81
		25 :0					1419.81	1419.81		
		26 :0					1433.84	1433.83		
		27 :0					1447.81	1447.84		
	t18 :1	**h21 :1**					1377.77	1377.73		
		h21:0					1379.79	1379.75	1421.81	1421.76
		h22 :0					1393.79	1393.76	1435.84	1435.77
		h23 :1			1406.79	1406.74	1405.81	1405.76		
		h23 :0			1408.79	1408.76	1407.83	1407.78	1449.84	1449.79
		h24 :0			1422.79	1422.78	1421.81	1421.79		
		h25 :0					1435.84	1435.81		
		h26 :0					1449.84	1449.82		

(*Continues*)

Table 1. (Continued)

LCB	FA	*A. thaliana* leaves		*A. thaliana* cells		BY-2 cells		BY-2 cells	
		Experimental $[M-H]^-$	Theoretical $[M-H]^-$	Experimental $[M-H]^-$	Theoretical $[M-H]^-$	Experimental $[M-H]^-$	Theoretical $[M-H]^-$	Experimental $[M-H]^-$	Theoretical $[M-H]^-$
Series C structures				**Ara-Hex-Glc-GlcA-Ins-P-Cer**		**Ara-Hex-GlcN-GlcA-Ins-P-Cer**		**Ara-Hex-GlcNAc-GlcA-Ins-P-Cer**	
t18 :0	**22 :0**					1511.82	1511.82	1553.86	1553.83
	23 :0					1525.83	1525.84		
	24 :0					1539.86	1539.86		
	25 :0					1553.86	1553.87		
t18 :0	**h22 :0**					1527.81	1527.82		
	h24 :0					1555.85	1555.85		
t18 :1	**22 :0**					1509.84	1509.81		
	24 :0					1537.87	1537.84		
t18 :1	**h21 :0**					1511.82	1511.79		
	h22 :0					1525.83	1525.80		
	h23 :0					1539.86	1539.82		
	h24 :0					1553.86	1553.83		
Series D structures				**$(Ara)_2$-Hex-Glc-GlcA-Ins-P-Cer**		**Ara-$(Hex)_2$-GlcN-GlcA-Ins-P-Cer**		**Ara-$(Hex)_2$-GlcNAc-GlcA-Ins-P-Cer**	
t18 :0	**22 :0**					1673.91	1673.88	1715.92	1715.89
	23 :0					1687.90	1687.89		
	24 :0			1672.89	1672.88	1701.92	1701.91		
t18 :0	**h21 :0**							1717.92	1717.87
	h22 :0					1689.89	1689.87		
	h23 :1			1672.89	1672.84	1701.92	1701.87		
t18 :1	**22 :0**					1671.87	1671.86	1713.89	1713.87
	24 :0			1670.86	1670.87	1699.91	1699.89		
t18 :1	**h21 :0**					1673.91	1673.84	1715.92	1715.85
	h22 :0					1687.90	1687.86		
	h23 :1			1670.86	1670.83	1699.91	1699.86		
	h23 :0			1672.89	1672.84				
Series E structures				**$(Ara)_3$-Hex-Glc-GlcA-Ins-P-Cer**		**Ara-$(Hex)_3$-GlcN-GlcA-Ins-P-Cer**		**Ara-$(Hex)_3$-GlcNAc-GlcA-Ins-P-Cer**	
t18 :0	**22 :0**					1835.96	1835.93	1877.98	1877.94
	23 :0					1849.95	1849.95		
	24 :0			1804.94	1804.92	1863.99	1863.96		
	25 :0			1818.94	1818.94				
t18 :0	**h21 :0**							1879.99	1879.92
	h23 :1			1804.94	1804.89				

(*Continues*)

		h24 :1	1818.94	1818.90				
	t18 :1	**22 :0**			1833.94	1833.91		
		23 :0			1847.96	1847.93		
		24 :0	1802.93	1802.91	1861.99	1861.95		
	t18 :1	**h21 :0**			1835.96	1835.89	1877.98	1877.90
		h22 :0			1849.95	1849.91		
		h23 :1	1802.93	1802.87				
		h23 :0	1804.94	1804.89	1863.99	1863.92		
Series F structures			**$(Ara)_4$-Hex-Glc-GlcA-Ins-P-Cer**		**$(Ara)_2$-$(Hex)_3$-GlcN-GlcA-Ins-P-Cer**		**$(Ara)_2$-$(Hex)_3$-GlcNAc-GlcA-Ins-P-Cer**	
	t18 :0	**22 :0**			1968.04	1967.97		
		23 :0			1982.02	1981.99		
		24 :0	1936.98	1936.97	1995.99	1996.00		
		25 :0	1950.98	1950.98				
	t18 :0	**h23 :1**	1936.98	1936.93				
		h23 :0	1938.98	1938.95				
		h24 :1	1950.98	1950.95				
	t18 :1	**22 :0**			1966.04	1965.96		
		24 :0	1934.98	1934.95	1994.03	1993.99		
	t18 :1	**h21 :0**			1968.04	1967.94		
		h22 :0			1982.02	1981.95		
		h23 :1	1934.98	1934.91				
		h23 :0	1936.98	1936.93	1995.99	1995.97		
		h24 :0	1950.98	1950.95				

Abbreviations: LCB, long-chain base; FA, fatty acid; Glc, glucose; GlcA, glucuronic acid; Ins, inositol; Cer, ceramide; GlcN, glucosamine, GlcNAc, *N*-acetylglucosamine; Hex, hexose; Ara, arabinose.

(theoretical *m/z* 1260.72), as already shown by Markham *et al.*[14,21] A less intense species at *m/z* 1262.73 corresponds to a t18:0 h24:0 ceramide moiety. The other peaks of the A series were attributed on this basis, suggesting the presence of long-chain base t18:0 and t18:1 and fatty acid chains from 24:0 to 29:0 and h22:0 to h28:0. The presence of h16:0 can be noticed as already described.[14,21]

In *A. thaliana* cells, compounds belonging to series A exhibited the highest intensities. Overall, the same species were observed in *A. thaliana* leaves, but with different abundances. The most intense peak was found at *m/z* 1260.73 (hexose(R1:OH)-hexuronic acid-inositol-phosphoceramide having a t18:1 h24:0 ceramide moiety). Ions at *m/z* 1244.74 and 1246.75 were attributed to GIPCs with t18:1 24:0 and t18:0 24:0 ceramide moieties, respectively, suggesting the presence of non-hydroxylated VLCFA. The other peaks of the A series were attributed to species with LCBs t18:0 and t18:1, and fatty acid chains from 24:0 to 27:0 and h22:0 to h26:0.

Peaks from series B to F were attributed in the same way. For *A. thaliana* cell GIPCs, the ion at *m/z* 1422.79 has a mass difference of 162.06 Da with the t18:1 h24:0 species at *m/z* 1260.73 corresponding to the addition of a hexose (162.05 Da). The same 162 Da mass difference is observed between *m/z* 1246.75 (t18:0 24:0) and 1408.79. So, compounds belonging to series B were identified as hexose-hexose(R1:OH)-hexuronic acid-inositol-phosphoceramide with LCBs t18:0 and t18:1, and fatty acid chains from 24:0 to 26:0 and h23:0 to h26:0. The C series was not detected in the case of *A. thaliana* cells. The D series exists in only two species at *m/z* 1670.86 and 1672.89, corresponding to the addition of two pentose units (2 × 132 Da) to a t18:1 24:0 compound observed at *m/z* 1406.79 and a t18:0 24:0 compound at *m/z* 1408.79, respectively. Thus, the D series was attributed to (pentose)$_2$-hexose-hexose(R1:OH)-hexuronic acid-inositol-phosphoceramides. Further, peaks in series E and F were attributed to (pentose)$_3$-hexose-hexose(R1:OH)-hexuronic acid-inositol-phosphoceramide and (pentose)$_4$-hexose-hexose (R1:OH)-hexuronic acid-inositol-phosphoceramide with LCBs t18:0 and t18:1 and fatty acid chains from 24:0 to 26:0.

Similarly, in BY-2 cells, series A to F were identified as hexose (R1)-hexuronic acid-inositol-phosphoceramides (series A), hexose-hexose(R1)-hexuronic acid-inositol-phosphoceramides (series B), pentose-hexose-hexose(R1)-hexuronic acid-inositol-phosphoceramides (series C), pentose-(hexose)$_2$-hexose(R1)-hexuronic acid-inositol-phosphoceramides (series D), pentose-(hexose)$_3$-hexose(R1)-hexuronic acid-inositol-phosphoceramides (series E) and (pentose)$_2$-(hexose)$_3$-hexose(R1)-hexuronic acid-inositol-phosphoceramides (series F), with LCBs as t18:0 and t18:1, fatty acid chains from 20:0 to 27:0 and/or from h20 to h26, and R1 being an amine or an acetylamine.

These preliminary structure attributions were further confirmed by MS/MS experiments.

Identification by tandem mass spectrometry

MALDI-MS/MS

First, fragment ion spectra were obtained in the negative ion mode by MALDI-MS/MS fragmentation of singly charged $[M–H]^-$ precursor ions. As an example, fragment ion spectra for *m/z* 1260.73 (*A. thaliana* cells) and 1301.78 (BY-2 cells)

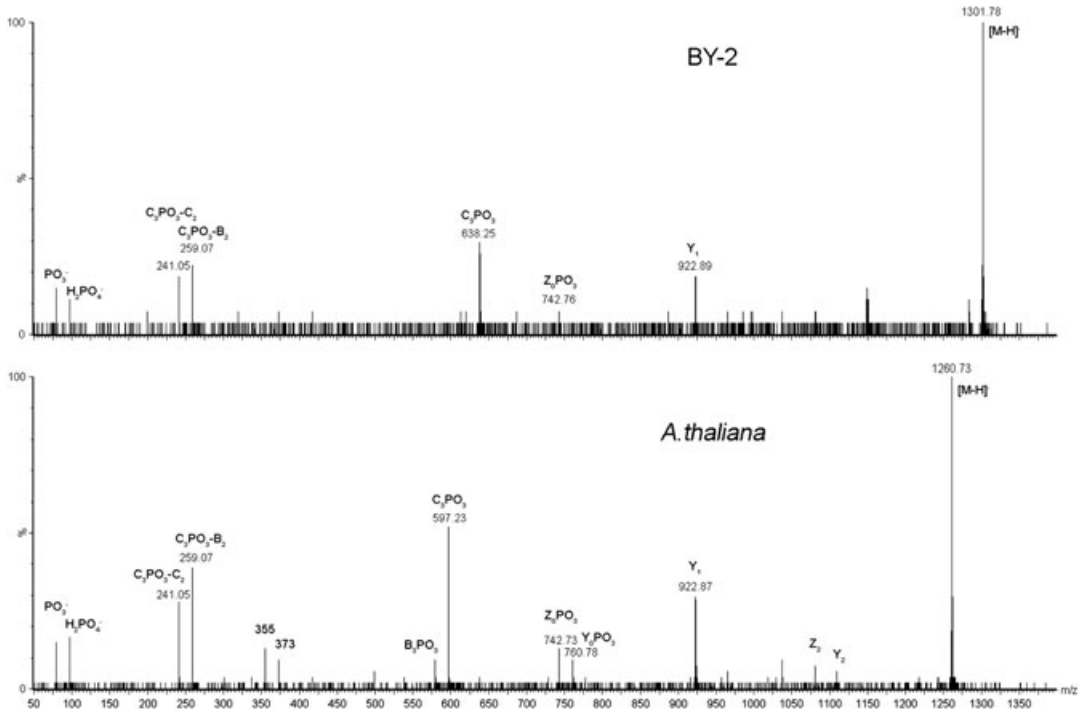

Figure 4. MALDI-MS/MS analysis of GIPCs from series A (BY-2 and *A. thaliana*). Collision-induced dissociation spectra were obtained from $[M–H]^-$ precursor ions at *m/z* 1301.78 (BY-2) and 1260.73 (*A. thaliana*). These ions correspond to hexose(R1)-hexuronic acid-inositol-phosphoceramide having a t18:1 h24:0 ceramide moiety with R1 being NAc and OH for BY-2 and *A. thaliana*, respectively. Argon was used as collision gas in a MALDI Q-ToF instrument; collision energy was set at −50 eV. Standard nomenclature for glycolipid fragmentation has been applied.[23,24]

Rapid Communications in Mass Spectrometry

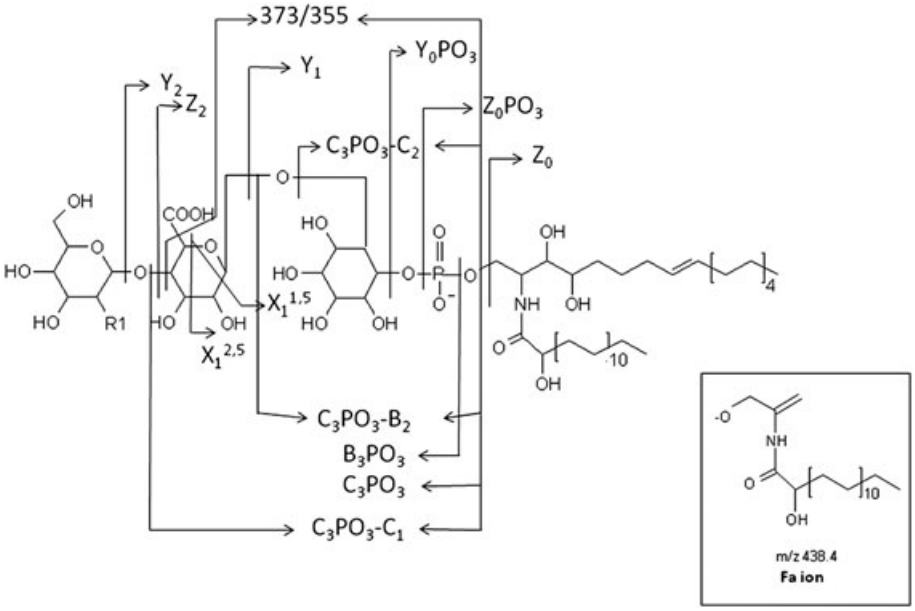

Figure 5. Characteristic fragmentations of GIPCs observed by MALDI- and ESI-MS/MS. Standard nomenclature for glycolipid fragmentation has been applied.[23,24] Hexose diastereomers and linkages are arbitrary. This GIPC structure corresponds to hexose (R1)-hexuronic acid-inositol-phosphoceramide having a t18:1 h24:0 ceramide moiety with R1 being NAc or NH_2 for BY-2 and OH for *A. thaliana*. Observed fragments and theoretical masses are paired in Table 1. A putative structure of the Fa ion is indicated.

precursor ions are presented in Fig. 4. The same fragment ion spectrum was obtained from the *m/z* 1260.72 precursor ion for *A. thaliana* leaves (not shown). Fragment ions were designated according to the nomenclature proposed by Costello and Vath[23] and Levery *et al.*;[24] characteristic ions are presented in a fragmentation scheme in Fig. 5. The presence of an inositol-phosphate moiety was attested by C_3PO_3-C_2 and C_3PO_3-B_2 ions, the presence of hexuronic acid was indicated by Y_2 or Z_2 ions, and the last carbohydrate turned out to be a hexose, as indicated by B_3PO_3 and C_3PO_3 ions. The ceramide moiety was identified by the Y_0PO_3 and Z_0PO_3 ions.

Two ions at *m/z* 373 and 355 were found in all GIPCs (series A to F); since their *m/z* values are not affected by changes in FA and LCB chains, these ions most likely contain the inositol group, in agreement with their theoretical masses (see Fig. 5 for a putative origin of these fragments). These internal ions, corresponding to hexuronic acid (without COOH)-inositol-phosphate, were not found in previous reports dealing with the fragmentation of positive ions,[21,23] and represent a signature of the polar head.

Noteworthy, some isobaric ceramide moieties could not be differentiated by MALDI-MS/MS. This is the case of a t18:1 h24:0 ceramide, isobaric with t18:0 h24:1 and t18:0 25:0. The ceramide moiety could also be d18:0 h25:0, but the proportion of d18 versus t18, as established by LCB analysis, is very low (about 5% and 10% for *A. thaliana* and BY-2 cells, respectively; Fig. 2(a)). Moreover, no signature ion of d18 was found in mass spectra, neither in MALDI-MS/MS nor in ESI-MS/MS (see further); consequently, the contribution of dihydroxylated species has been neglected in the present work. Finally, fragmentation of ions at *m/z* 1260.73 (*A. thaliana* cells) and 1301.78 (BY-2 cells) confirmed the identification of hexose (R1)-hexuronic acid-inositol-phosphoceramide, with R1 as a hydroxyl in *A. thaliana* cells and an acetylamine in BY-2 cells, the ceramide moiety being t18:1 h24:0, t18:0 h24:1 or t18:0 25:0. A mixture of isomers might be present under the same peak, but the species with the t18:1 h24:0 ceramide moiety seemed to be the major ones, in agreement with the distribution presented in Fig. 2.

Attempts to achieve MALDI-MS/MS fragment ion analysis for series B to F were mostly unsuccessful because of the weak intensity of precursor ions. Therefore, to complete the identifications within these series, MS/MS experiments were carried out in the ESI mode with a QTRAP instrument.

ESI-MS/MS

ESI-MS/MS was achieved in the negative ion mode with doubly charged precursor ions $[M–2H]^{2–}$ from series A. As an example, the fragment ion spectra of precursors at *m/z* 629.85 (*A. thaliana* cells) and 650.30 (BY-2 cells) are presented in Fig. 6 (data not shown for *A. thaliana* leaves). Characteristic ions are reported in the fragmentation scheme (Fig. 5).[23,24] As in the case of MALDI-MS/MS spectra, evidence of the presence of an inositol-phosphate moiety is found with C_3PO_3-C_2 and C_3PO_3-B_2 ions and Y_2/Z_2 ions indicate the presence of hexuronic acid. The B_3PO_3 and C_3PO_3 ions are absent, but the last carbohydrate (a hexose in the present case) can be identified by calculating the mass difference between the pseudo-molecular ion and the Y_2 fragment. The ceramide moiety was identified with Y_0PO_3, Z_0PO_3 and Z_0 ions. Ions at *m/z* 373 and 355 that characterize the polar head are also found in ESI mode. Another fragment ion characteristic of the negative ion mode appears in these spectra at *m/z* 438.3. We observed that its *m/z* value increased by 14 Da when the

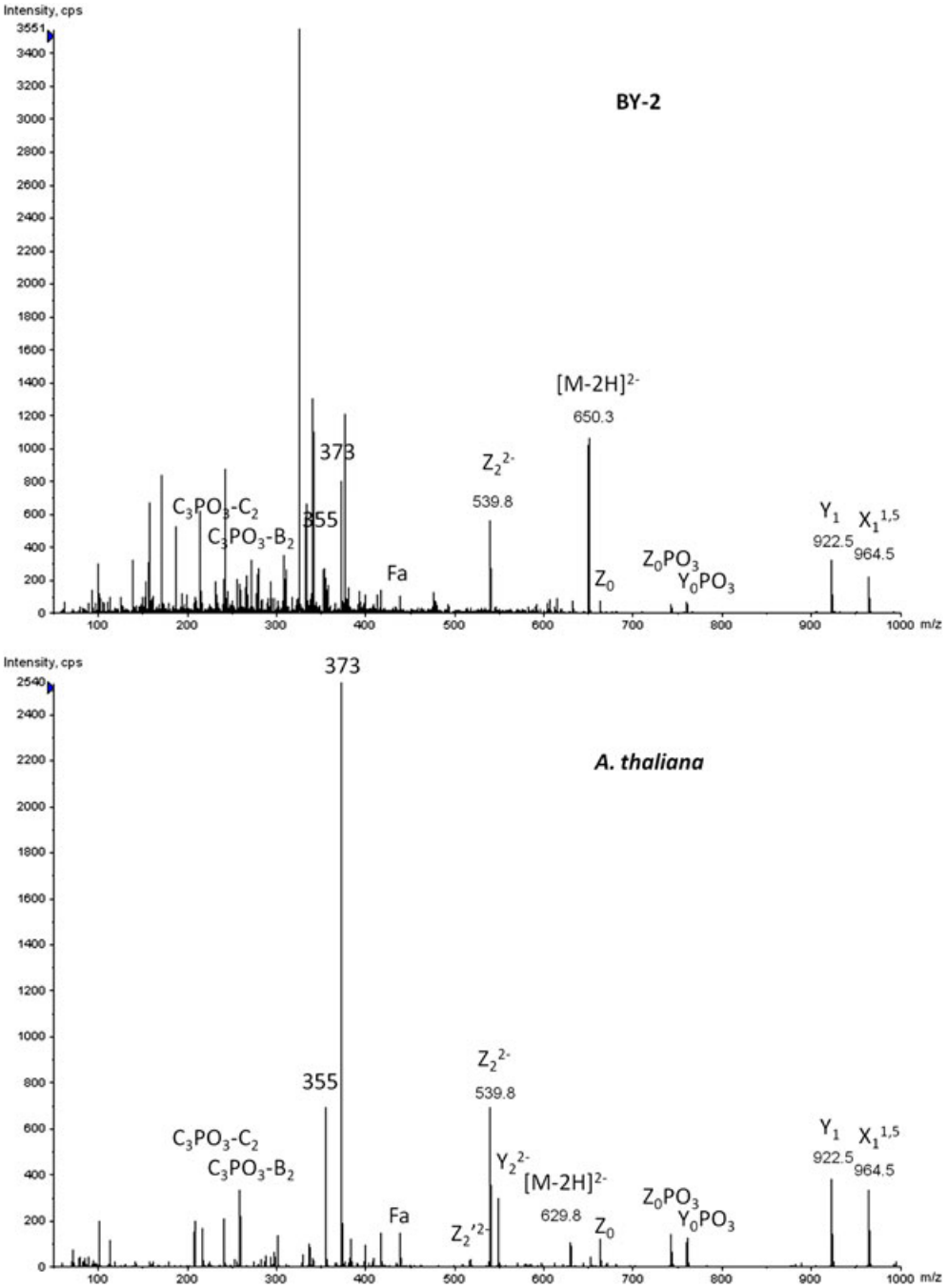

Figure 6. ESI-MS/MS analysis of GIPCs from series A (BY-2 and *A. thaliana*). Collision-induced dissociation spectra were obtained from $[M–2H]^{2–}$ ions at *m/z* 650.30 (BY-2) and 629.85 (*A. thaliana*). These ions correspond to hexose(R1)-hexuronic acid-inositol-phosphoceramide having a t18:1 h24:0 ceramide moiety with R1 being NAc and OH for BY-2 and *A. thaliana*, respectively. Nitrogen was used as collision gas in a QTRAP instrument, with the collision energy set to −40 eV. Standard nomenclature for glycolipid fragmentation has been applied.[23,24]

precursor ion mass was also increased by 14 Da. Thus, this ion was likely correlated to the fatty acid chain length; a putative structure is indicated in Fig. 5, in agreement with its calculated *m/z* value. We named this ion Fa. In the case of spectra shown in Fig. 6, the Fa ion allowed identification of the fatty acid chain as h24:0. However, the Fa ion did not allow the assignment of ceramides with dihydroxylated LCBs.

Confirming the results obtained in the MALDI mode, the ceramide moieties of GIPCs belonging to series A were identified by ESI-MS/MS as hexose(R1)-hexuronic acid-inositol-phosphoceramide(t18:1 h24:0), the R1 group being a hydroxyl function in *A. thaliana* and an acetylamine in BY-2 cells.

Owing to a better sensitivity in ESI-MS/MS mode, we could also fragment other GIPC series and confirm preliminary structure assignments. However, the Fa ion was not

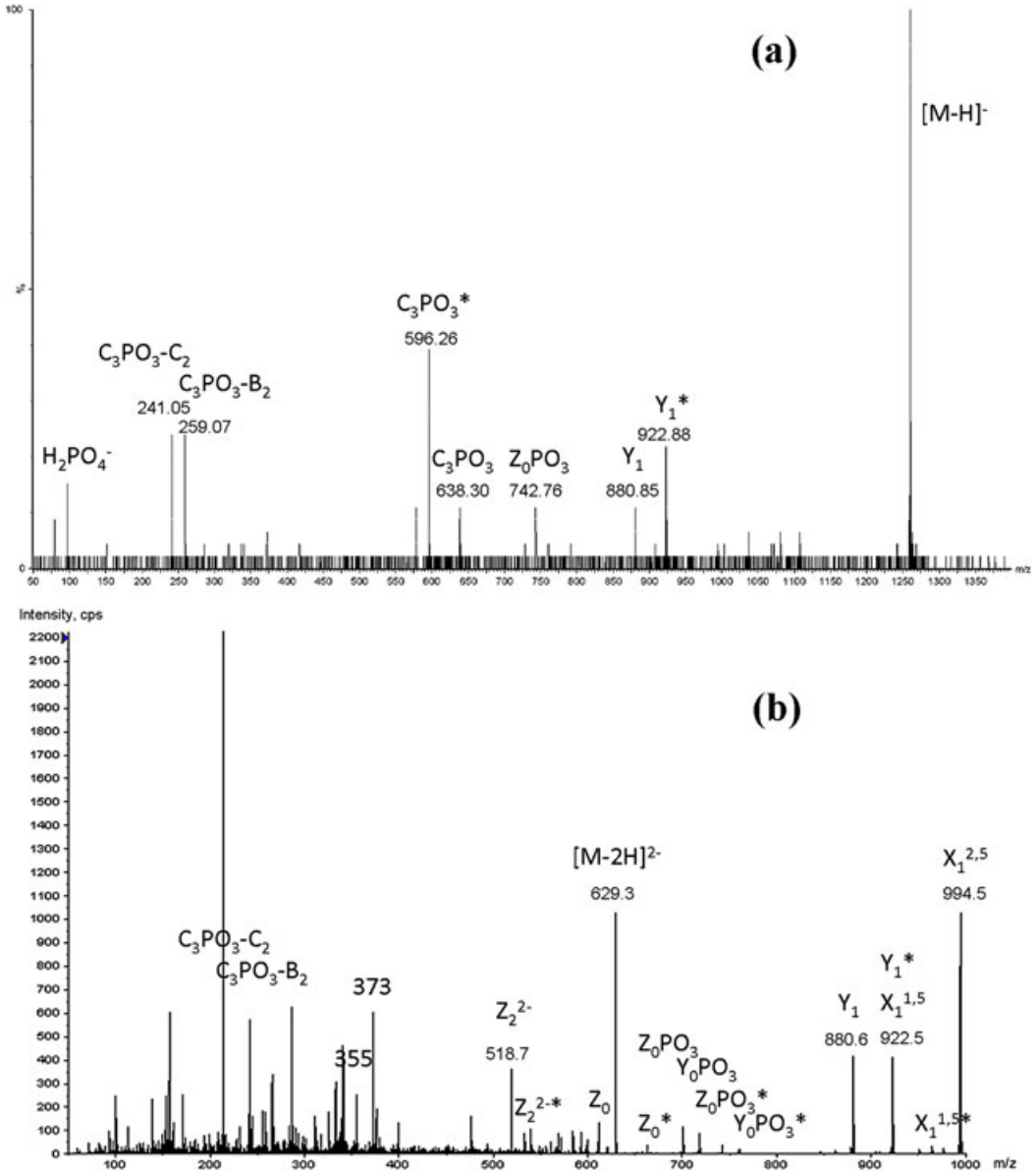

Figure 7. MS/MS analysis of isobaric species in BY-2 cells. (a) MALDI. Fragmentation of the $[M–H]^-$ ion at *m/z* 1259.76. Argon was used as collision gas in a MALDI Q-ToF instrument with the collision energy set to −50 eV. (b) ESI. Fragmentation of the $[M–2H]^{2-}$ ion at *m/z* 629.38. Nitrogen was used as collision gas in a QTRAP instrument with the collision energy set to −40 eV. The structures of the isobaric species correspond to hexose(R1)-hexuronic acid-inositol-phosphoceramide having a t18:1 h24:0 ceramide moiety with R1 being NH_2 and hexose(R1)-hexuronic acid-inositol-phosphoceramide having a t18:1 h21:0 ceramide moiety with R1 being NAc. Standard nomenclature for glycolipid fragmentation has been applied.[23,24] Ions from isobaric species are labeled with an asterisk.

always observed, preventing the identification of some ceramide moieties. Nevertheless, isobaric species occurring in BY-2 cells could be identified.

Identification of isobaric species in BY-2 cells by MS/MS

Tandem mass spectra of BY-2 GIPCs (MALDI-MS/MS for the $[M–H]^-$ precursor ion at *m/z* 1259.76, and ESI-MS/MS for the $[M–2H]^{2-}$ precursor ion at *m/z* 629.38) are shown in Figs. 7(a) and 7(b). For both MALDI and ESI modes, some fragment ions (Z_2, $X_1^{2,5}$, $X_1^{1,5}$, Y_1, Y_0PO_3, Z_0PO_3, Z_0) appear as doublets having a mass difference of 42 Da from the Z_2*, $X_1^{1,5}$*, Y_1*, Y_0PO_3*, Z_0PO_3* and Z_0* ions. Thus, these ion doublets are likely related to the addition of three methylene units on the fatty acid chain.

A similar doublet, which appeared only on MALDI-MS/MS spectra, was observed with the C_3PO_3 ion (42 Da difference with the C_3PO_3* ion). In this case, the structural difference was located on the R1 group of the last sugar unit of the carbohydrate moiety: R1 is either an amine or an acetylamine, and this 42 Da difference is balanced by the

fatty acid chain length (C_{n-3} or C_n). Thus, the isobaric species could be identified as hexose(NH_2)-hexuronic acid-inositol-phosphoceramide (t18:1 h24:0) and hexose(NAc)-hexuronic acid-inositol-phosphoceramide(t18:1 h21:0).

DISCUSSION

The method developed earlier by Carter and Koob works well for isolation of plant GIPCs.[10] After modifications made in order to get rid of proteins and select an appropriate solvent, it became perfectly suited to mass spectrometric analysis in MALDI and ESI ionization modes. MALDI-MS in the negative ion mode with DHA matrix reveals the distribution of plant GIPC series at a glance (Fig. 3). Whereas the positive ion mode is still often used in MALDI- and ESI-MS for the analysis of GIPCs,[14,21,23] we found a clear advantage in using the negative ion mode with our sample preparation, because it did not lead to sodium and potassium adduct forms and revealed the occurrence of highly glycosylated GIPCs for *A. thaliana* and BY-2 cell samples. However, the quick overview obtained by full scan MALDI-MS is not sufficient for the assignment of all GIPC structures. A Q-ToF instrument provides a narrow isolation width of precursor ions, and accurate mass measurements for both precursor and fragment ions, two features that are particularly useful for a safe structural assignment of plant GIPCs by means of MALDI-MS/MS. Fragmentation patterns obtained by MALDI-MS/MS and ESI-MS/MS were similar. However, complementary information was also derived from these two modes, since the C_3PO_3 ion representative of the carbohydrate moiety was only obtained by MALDI-MS/MS and the Fa ion, representative of the ceramide moiety, was only obtained by ESI-MS/MS. When present, the Fa ion allowed identification of the fatty acid chain of the ceramide moiety. Furthermore, ions at *m/z* 373 and 355 observed in the negative ion mode represent a useful signature of the polar head.

Mass differences between GIPC series A to F were found to be either 162 or 132 Da, corresponding to additional hexose or pentose units. In agreement with this observation, previously identified saccharides in *Arabidopsis* leaves were mostly galactose and arabinose, whereas galactose, mannose and arabinose were found in tobacco leaves; in both species, hexuronic acid was identified as glucuronic acid.[4,13,15]

Since pure reference compounds were not available at this stage of the work, relative abundances of GIPC series could not be assessed on the basis of full scan MALDI mass spectra, and should be taken as a rough indication of real GIPC distribution in series having increasing numbers of sugar units. For *A. thaliana* cells and leaves (Figs. 3(b) and 3(c), respectively), series A was largely predominant on MALDI-MS spectra, whereas main series were A, B and E for BY-2 cells (Fig. 3(a)), i.e. GIPC species bearing two, three and six sugars, respectively. These results are in agreement with those reported by Markham *et al*., who also found compounds of series A in *A. thaliana* leaves, and weak signals for compounds of the B series,[14] and with the work of other research groups who reported the occurrence of several GIPC series in tobacco leaves.[4,13,15]

A majority of 2-hydroxylated VLCFAs (including h16:0) and t18:1 LCB were found in *A. thaliana* leaves (Fig. 2), in accordance with Markham *et al*.[14,21] However, this latter research group did not report on the occurrence of non-hydroxylated VLCFAs that we found in low amounts. This difference can be related to the detection method, since Markham *et al*. used a MRM-based method.[21]

Extracts from *A. thaliana* leaves and cells display globally the same GIPC species, but in different proportions (Fig. 2 and Table 1). For example, in leaves, the most intense peaks were found at *m/z* 1258.71 (t18:1 h24:1 ceramide moiety) and 1260.72 (t18:1 h24:0 ceramide moiety), whereas in cells the most intense peaks were at *m/z* 1260.73 (t18:1 h24:0 ceramide moiety) and 1262.75 (t18:0 h24:0 ceramide moiety). The acyl group h16:0 was found in both cases (Table 1). However, some differences are noticeable. Firstly, the huge proportion of t18:0 in cells compared to leaves illustrates the differences between cell and leaf biological models. Secondly, the presence of ions at *m/z* 1244.74 (t18:1 24:0 ceramide moiety) and 1246.75 (t18:0 24:0 ceramide moiety) attested the presence of non-hydroxylated VLCFAs in cells, as corroborated by GC/MS analysis (Fig. 2), but these compounds were present in low amounts in leaves. In *A. thaliana* cells and leaves and BY-2 cells, we found evidence for the occurrence of fatty acid chains with odd and even carbon numbers in mass spectra (Fig. 3 and Table 1), whereas Markham *et al*. found several sphingolipids from *Arabidopsis* differing by 28 Da, indicating fatty acid chains with even carbon number only.[14,21] The occurrence of fatty acid chains with odd carbon numbers has been confirmed by GC/MS analysis of FAMEs (Fig. 2(b)), and is in agreement with fatty acid chain distributions reported for *Aspergillus fumigatus* and *Nicotiana tabacum*.[15,25]

Tandem mass spectra have highlighted differences in the GIPC structures from *Arabidopsis* and BY-2 cells. In the two cell types, series A and B only bear hexoses. However, series D to F correspond to the addition of several pentose units for *A. thaliana* cells, and to the addition of several hexoses and one pentose for BY-2 cells. While in *A. thaliana* cells R1 is a hydroxyl group,[5] it can be either an amine or an acetylamine in BY-2 cells.[5,13] In the BY-2 sample, isobaric GIPC species have been differentiated with the help of MS/MS spectra. In this particular case, the mass difference arising from the R1 substituent was balanced by a difference of three carbon atoms in the length of the fatty acid chain.

MALDI-MS/MS turned out to be a quick way to access detailed characterization of plant GIPCs, thereby opening new avenues to decipher structure–function relationships between glycosphingolipids and membrane organization, and to define the involvement of GIPCs in host–pathogen interactions.

Acknowledgements

We acknowledge funding of the French Agence Nationale de la Recherche programme blanc 'PANACEA' NT09_517917 (contracts to SM and JMS), of the Région Aquitaine and of platforms Métabolome-Lipidome-Fluxome of Bordeaux (https://www.bordeaux.inra.fr/umr619/RMN_index.htm) and Protéome (http://www.pgfb.u-bordeaux2.fr/proteome/index.html), for contribution to mass spectrometry equipment.

Rapid Communications in Mass Spectrometry

REFERENCES

[1] H. E. Carter, R. H. Gigg, J. H. Law, T. Nakayama, E. Weber. Biochemistry of the sphingolipids. XI. Structure of phytoglycolipid. *J. Biol. Chem.* **1958**, *233*, 1309.

[2] S. Spassieva, J. Hille. Plant sphingolipids today – are they still enigmatic? *Plant Biol.* **2003**, *5*, 125.

[3] D. Worrall, C. K. Ng, A. M. Hetherington. Sphingolipids, new players in plant signaling. *Trends Plant Sci.* **2003**, *8*, 317.

[4] D. V. Lynch, T. M. Dunn. An introduction to plant sphingolipids and a review of recent advances in understanding their metabolism and function. *New Phytol.* **2004**, *161*, 677.

[5] R. A. Laine, T. C. Y. Hsieh. *Inositol-containing sphingolipids. Methods Enzymol.* **1987**, *138*, 186.

[6] S. Perotto, N. Donovan, B. K. Drobak, N. J. Brewin. Differential expression of a glycosyl inositol phospholipid antigen on the peribacteroid membrane during pea nodule development. *Mol. Plant Microbe Interact.* **1995**, *8*, 560.

[7] L. M. Obeid, Y. Okamoto, C. Mao. Yeast sphingolipids: metabolism and biology. *Biochim. Biophys. Acta* **2002**, *1585*, 163.

[8] D. Warnecke, E. Heinz. Recently discovered functions of glucosylceramides in plants and fungi. *Cell. Mol. Life Sci.* **2003**, *60*, 919.

[9] P. Sperling, S. Franke, S. Luthje, E. Heinz. Are glucocerebrosides the predominant sphingolipids in plant plasma membranes? *Plant Physiol. Biochem.* **2005**, *43*, 1031.

[10] H. E. Carter, J. L. Koob. Sphingolipid in bean leaves (*Phaseolus vulgaris*). *J. Lipid Res.* **1969**, *10*, 363.

[11] K. Kaul, R. L. Lester. Characterization of inositol-containing phosphosphingolipids from tobacco leaves: Isolation and identification of two novel, major lipids: N-acetylglucosamidoglucuronidoinositol phosphorylceramide and glucosamidoglucuronidoinositol phosphorylceramide. *Plant Physiol.* **1975**, *55*, 120.

[12] T. C. Hsieh, K. Kaul, R. A. Laine, R. L. Lester. Structure of a major glycophosphoceramide from tobacco leaves, PSL-I: 2-deoxy-2-acetamido-D-glucopyranosyl(alpha1 leads to 4)-D-glucuronopyranosyl(alpha1 leads to 2)myoinositol-1-O-phosphoceramide. *Biochemistry* **1978**, *17*, 3575.

[13] T. C. Hsieh, R. L. Lester, R. A. Laine. Glycophosphoceramides from plants. Purification and characterization of a novel tetrasaccharide derived from tobacco leaf glycolipids. *J. Biol. Chem.* **1981**, *256*, 7747.

[14] J. E. Markham, J. Li, E. B. Cahoon, J. G. Jaworski. Separation and identification of major plant sphingolipid classes from leaves. *J. Biol. Chem.* **2006**, *281*, 22684.

[15] M. O. Pata, Y. A. Hannun, C. K. Y. Ng. Plant sphingolipids: decoding the enigma of the Sphinx. *New Phytol.* **2010**, *185*, 611.

[16] N. F. Keinath, S. Kierszniowska, J. Lorek, G. Bourdais, S. A. Kessler, H. Shimosato-Asano, U. Grossniklaus, W. X. Schulze, S. Robatzek, R. Panstruga. PAMP (pathogen-associated molecular pattern)-induced changes in plasma membrane compartmentalization reveal novel components of plant immunity. *J. Biol. Chem.* **2010**, *285*, 39140.

[17] T. Stanislas, D. Bouyssie, M. Rossignol, S. Vesa, J. Fromentin, J. Morel, C. Pichereaux, B. Monsarrat, F. Simon-Plas. Quantitative proteomics reveals a dynamic association of proteins to detergent-resistant membranes upon elicitor signaling in tobacco. *Mol. Cell. Proteomics* **2009**, *8*, 2186.

[18] J. Morel, S. Claverol, S. Mongrand, F. Furt, J. Fromentin, J. J. Bessoule, J. P. Blein, F. Simon-Plas. Proteomics of plant detergent-resistant membranes. *Mol. Cell. Proteomics* **2006**, *5*, 1396.

[19] E. Bayer, C. L. Thomas, A. J. Maule. Plasmodesmata in *Arabidopsis thaliana* suspension cells. *Protoplasma* **2004**, *223*, 93.

[20] G. Bonaventure, J. J. Salas, M. R. Polar, J. B. Ohlrogge. Disruption of the FATB gene in *Arabidopsis* demonstrates an essential role of saturated fatty acids in plant growth. *Plant Cell* **2003**, *15*, 1020.

[21] J. E. Markham, J. G. Jaworski. Rapid measurement of sphingolipids from *Arabidopsis thaliana* by reversed-phase high-performance liquid chromatography coupled to electrospray ionization tandem mass spectrometry. *Rapid Commun. Mass Spectrom.* **2007**, *21*, 1304.

[22] B. Colsch, A. S. Woods. Localization and imaging of sialylated glycosphingolipids in brain tissue sections by MALDI mass spectrometry. *Glycobiology* **2010**, *20*, 661.

[23] C. E. Costello, J. E. Vath. Tandem mass spectrometry of glycolipids. *Methods Enzymol.* **1990**, *193*, 738.

[24] S. B. Levery, M. S. Toledo, A. H. Straus, H. K. Takahashi. Comparative analysis of glycosylinositol phosphorylceramides from fungi by electrospray tandem mass spectrometry with low-energy collision-induced dissociation of Li^+ adduct ions. *Rapid Commun. Mass Spectrom.* **2001**, *15*, 2240.

[25] C. Simenel, B. Coddeville, M. Delepierre, J. P. Latgé, T. Fontaine. Glycosylinositolphosphoceramides in *Aspergillus fumigatus*. *Glycobiology* **2008**, *18*, 84.

